Reconsideration of the lattice effect on the charge-ordering transition of doped manganites

A. Machida
Department of Crystalline Materials Science, Nagoya University, Nagoya 464-8603, Japan

Y. Moritomo
CIRSE, Nagoya University, Nagoya 464-8601, Japan
and PRESTO, JST, Tokyo 102, Japan

K. Ohoyama, S. Okamoto, S. Ishihara, and S. Maekawa
Institute for Materials Research, Tohoku University, Sendai 980-8577, Japan

A. Nakamura
CIRSE, Nagoya University, Nagoya 464-8601, Japan
(Received 16 March 2000)

On the basis of the neutron structural analysis, lattice effect on the charge/orbital-ordering transition of doped manganites has been reconsidered. We have investigated the stability of the respective e_g orbitals by a Madelung potential calculation, and have found a close correlation between the orbital stability and the charge-ordering transition. This observation indicates that the chemical pressure has an aspect of orbital control, besides the control of the transfer integral t between the neighboring Mn sites.

Perovskite-type doped manganites $R_{1-x}A_xMnO_3$ where R and A are trivalent rare-earth and divalent alkaline-earth ions, respectively, have three-dimensional networks of the MnO_6 octahedra. Variation of the averaged ionic radius $\langle r_A \rangle$ of the perovskite A site modifies the Mn-O-Mn angle, bond length, and so on, and affects the magnetotransport properties. Among the lattice structural changes induced by *chemical pressure*, the variation of the Mn-O-Mn angle Θ has been focused. This is because suppression of the Curie temperature T_C with decrease of $\langle r_A \rangle$ has been ascribed to the reduced transfer integral $t[\propto \sin(\Theta/2)]$ between the Mn sites. Radaelli *et al.*[1] have experimentally confirmed this trend at a fixed $x(=0.3)$. On the other hand, a chemical pressure effect for the layered manganites $(R,A)_{n+1}Mn_nO_{3n+1}$ $(n=1,2)$ is different from that for the cubic perovskite. Moritomo *et al.*[2] have observed suppression of the charge/orbital-ordering temperature of single-layer $La_{0.5}Sr_{1.5}MnO_4$ with substitution of the Nd^{3+} ions for La^{3+} ions, and have ascribed it to the elongated MnO_6 octahedra and resultant unstabilized $d_{3x^2-r^2}/d_{3y^2-r^2}$ orbital alternation. Akimoto *et al.*[3] have found a correlation between the orbital stability at room temperature and magnetic structures in the structure-controlled bilayer manganites at a fixed $x(=0.4)$. These experimental observations indicate that the chemical pressure effects in the layered manganites have an aspect of the *orbital control*.

The charge-ordering transition of the cubic manganites, e.g., $Nd_{1/2}Sr_{1/2}MnO_3$,[4] accompanies an antiferromagnetic spin ordering with the CE-type structure,[5–7] as well as the $d_{3x^2-r^2}/d_{3y^2-r^2}$ orbital alternation. Such an orbital-ordered state has been observed by anisotropy of the tensor of susceptibility scattering measurement in $Nd_{1/2}Sr_{1/2}MnO_3$ (Ref. 8) as well as by the electron microscope in $La_{1/2}Ca_{1/2}MnO_3$.[9] The chemical pressure effect on the charge-ordering transition has been regarded as control of t with change of $\langle r_A \rangle$: the smaller t becomes, the more stable the charge-ordered state becomes.[10] However, we know a serious exception on this trend. In $(Nd_{1-y}Sm_y)_{1/2}Sr_{1/2}MnO_3$,[11] the charge-ordering temperature T_{CO} is ~ 150 K at $y=0$ ($\langle r_A \rangle = 1.355$ Å), but the transition disappears at $y=0.84$ ($\langle r_A \rangle = 1.342$ Å) even though the value of t is fairly suppressed. Judging from the fact that the charge-ordering transition accompanies the orbital alternation, variation of the orbital stability induced by the chemical pressure should affect the charge-ordering transition. Here, we have investigated stability of the respective e_g orbitals by means of Madelung potential calculations based on the structural data at room temperature obtained by neutron powder diffraction experiments. We have found a close correlation between the orbital stability at room temperature and the ground state, indicating that the orbital stability governs the charge-ordering transition of the half-doped manganites.

A series of ceramics compounds $R_{1/2}A_{1/2}MnO_3$ ($R=$ La, Pr, Nd, $Nd_{1/2}Tb_{1/2}$, and Tb, $A=$ Sr and Ca), was synthesized by solid-state reaction in air atmosphere. Stoichiometric mixture of commercial La_2O_3, Pr_2O_3, Nd_2O_3, Tb_4O_7, $SrCO_3$, $CaCO_3$, and Mn_3O_4 powder was well ground and calcined two times at 1250–1350°C for 24 h. Then, the resulting powder was pressed into a disk with a size of 20 mm $\phi \times 4$ mm and sintered at 1250–1350 °C for 24 h. Rietveld analysis[12] of neutron powder patterns indicates that investigated compounds were single phase without detectable impurities. The crystal symmetry is ortho rhombic ($Pbnm; Z=4$) except for $La_{1/2}Sr_{1/2}MnO_3$, $(La_{1/2}Nd_{1/2})_{1/2}Sr_{1/2}MnO_3$, $Pr_{1/2}Sr_{1/2}MnO_3$, and $Nd_{1/2}Sr_{1/2}MnO_3$ ($Ibmm; Z=4$). Neutron powder diffraction measurements were performed with the Kinken powder diffractometer for high efficiency and high-resolution measurements[13] (HERMES) installed at the JRR-3M reactor at the Japan Atomic Energy Research Institute, Tokai, Japan. Neutrons with wavelength 1.8196 Å were obtained by the 331 reflection of the Ge monochromator, and 12′-∞-Sample-22′ collimation.

TABLE I. Lattice constants and atomic positions for $R_{1/2}A_{1/2}MnO_3$ determined from neutron powder profiles at room temperature. g means oxygen occupancy determined by Rietveld analysis. The crystal symmetry is orthorhombic [$Ibmm, Z=4$ for $La_{1/2}Sr_{1/2}MnO_3$, $(La_{1/2}Nd_{1/2})_{1/2}Sr_{1/2}MnO_3$, $Pr_{1/2}Sr_{1/2}MnO_3$, and $Nd_{1/2}Sr_{1/2}MnO_3$, and $Pbnm, Z=4$ for other samples]. The atomic sites are $R/A, 4e[x,0,\frac{1}{4}]$, Mn, $4b[\frac{1}{2},0,0]$, O(1), $4e[x,\frac{1}{2},\frac{1}{4}]$, O(2), $8g[\frac{1}{4},\frac{3}{4},z]$ for *Ibmm* symmetry and $R/A, 4c[x,y,\frac{1}{4}]$, Mn, $4b[\frac{1}{2},0,0]$, O(1), $4c[x,y,\frac{1}{4}]$, O(2), $8d[x,y,z]$ for *Pbnm* symmetry. T_C and T_{CO} are the Curie and charge-ordering temperatures, respectively.

	a (Å)	b (Å)	c (Å)	R_{wp} (%)	T_C (K)	T_{CO} (K)	g
$La_{1/2}Sr_{1/2}MnO_3$	5.4412(5)	5.4418(5)	7.7643(2)	7.97	360		1.021(5)
$(La_{1/2}Nd_{1/2})_{1/2}Sr_{1/2}MnO_3$	5.4783(3)	5.4512(3)	7.6654(3)	7.36	305[a]		0.991(5)
$Pr_{1/2}Sr_{1/2}MnO_3$	5.413(1)	5.408(1)	7.7541(6)	3.16	265[6]		0.981(7)
$Nd_{1/2}Sr_{1/2}MnO_3$	5.4405(2)	5.3986(2)	7.5832(3)	6.36	265	150	0.999(5)
$(Nd_{1/2}Tb_{1/2})_{1/2}Sr_{1/2}MnO_3$	5.4104(8)	5.3990(8)	7.6052(6)	5.98	280[b]		0.944(6)
$Tb_{1/2}Sr_{1/2}MnO_3$	5.4051(7)	5.4078(7)	7.6159(4)	3.58			0.999(3)
$La_{1/2}Ca_{1/2}MnO_3$	5.4243(3)	5.4156(3)	7.6334(2)	6.19	230	140	1.017(4)
$Nd_{1/2}Ca_{1/2}MnO_3$	5.3815(2)	5.4026(2)	7.5974(2)	5.24		223	1.006(4)
$(Nd_{1/2}Tb_{1/2})_{1/2}Ca_{1/2}MnO_3$	5.3565(3)	5.4156(3)	7.5505(4)	5.38		240	1.001(5)
$Tb_{1/2}Ca_{1/2}MnO_3$	5.3206(2)	5.4449(2)	7.4477(3)	5.63		289	1.000(5)

R/A		O(1)		O(2)		
x	y	x	y	x	y	z
0.018(1)		0.966(1)				0.0050(8)
−0.0006(9)		0.9572(7)				0.0215(3)
−0.026(3)		0.060(2)				−0.008(1)
0.0018(6)		0.9460(6)				0.0245(3)
−0.003(2)	0.017(1)	0.945(2)	0.496(2)	0.227(2)	0.767(2)	0.0304(6)
0.002(2)	0.0240(8)	0.940(2)	0.492(2)	0.220(2)	0.775(2)	0.0331(6)
0.0011(9)	0.0184(5)	0.9417(7)	0.4907(7)	0.2247(6)	0.7774(6)	0.0310(3)
0.0045(8)	0.0316(4)	0.9331(8)	0.4894(5)	0.2138(4)	0.7859(4)	0.0364(3)
0.0055(9)	0.0400(5)	0.9297(8)	0.4845(6)	0.2102(5)	0.7903(5)	0.0399(3)
0.0098(5)	0.0504(5)	0.9175(5)	0.4803(5)	0.2066(3)	0.7938(4)	0.0423(2)

[a]*A*-type antiferromagnetic metallic phase appears at low temperature. (Ref. 19).

[b]The magnetization at low temperature ($\sim 1\mu_B$ under 0.5 T) is much smaller than the ideal value ($=3.5\ \mu_B$).

Figure 1 shows temperature dependence of (a) activation energy $E_{ac}[\equiv d(\ln\rho)/d(1/T)$, where ρ is resistivity] and (b) susceptibility χ for $R_{1/2}A_{1/2}MnO_3$. For four-probe resistivity measurements, the sample was cut into a rectangular shape, typically of $3\times2\times1$ mm^3, and electrical contacts were made with a heat-treatment-type silver paint. The E_{ac}-T curve of $Tb_{1/2}Ca_{1/2}MnO_3$ has a peak at $\approx$289 K due to the charge-ordering transition. The transition temperature T_{CO} was defined as the maximal point (downward arrow) of the E_{ac}-T curve. In the case of Ca compounds (solid curves), T_{CO} decreases with increase of $\langle r_A\rangle$: $T_{CO}\approx$289 K (Ref. 14) for $Tb_{1/2}Ca_{1/2}MnO_3(\langle r_A\rangle=1.270$ Å), $\approx$223 K for $Nd_{1/2}Ca_{1/2}MnO_3(\langle r_A\rangle=1.305$ Å), and $\approx$140 K for $La_{1/2}Ca_{1/2}MnO_3(\langle r_A\rangle=1.350$ Å). This trend is consistent with the recent work done by Fontcuberta *et al.*[15] The charge-ordering transition accompanies the CE-type spin-ordering, which causes the reduction of the χ-T curve. Figure 1(b) shows the χ-T curves for $R_{1/2}A_{1/2}MnO_3$. χ was measured under a field of $\mu_0H=0.5$ T after cooling down to 5 K in the zero field (ZFC), using a superconducting quantum interference device magnetometer.

Curiously enough, there is no trace of the charge-ordering transition in the E_{ac}-T curve of $Tb_{1/2}Sr_{1/2}MnO_3$ [$\langle r_A\rangle=1.320$ Å; broken curve of Fig. 1(a)], and the curve monotonously decreases with decrease of temperature. In addition, the χ-T curve of $Tb_{1/2}Sr_{1/2}MnO_3$ shows Curie-Weiss behavior down to $\sim$40 K [broken curve of Fig. 1(b)]. Similarly, there is no trace of the charge-ordering transition in $(Nd_{1/2}Tb_{1/2})_{1/2}Sr_{1/2}MnO_3$ ($\langle r_A\rangle=1.338$ Å; not shown). Sundaresan *et al.*[16] and Kasper *et al.*[17] have investigated magnetic properties of $R_{1-x}Sr_xMnO_3$ (R=Eu, Gd, Tb, Dy and Y) at $x\simeq0.5$, and have observed spin-glass behavior at low temperature.[18] We think that the low-temperature spin state of $Tb_{1/2}Sr_{1/2}MnO_3$ and $(Nd_{1/2}Tb_{1/2})_{1/2}Sr_{1/2}MnO_3$ is also spin-glass-like. Looking at Table I, T_{CO} is $\approx$223 K for $Nd_{1/2}Ca_{1/2}MnO_3(\langle r_A\rangle=1.305$ Å) and $\approx$140 K for $La_{1/2}Ca_{1/2}MnO_3(\langle r_A\rangle=1.350$ Å). So, we could expect the charge-ordering transition at $\sim$200 K for $Tb_{1/2}Sr_{1/2}MnO_3(\langle r_A\rangle=1.320$ Å) and $(Nd_{1/2}Tb_{1/2})_{1/2}Sr_{1/2}MnO_3(\langle r_A\rangle=1.338$ Å), if the transition were governed by the $\langle r_A\rangle$ value.

Now, let us proceed to the overall structural feature of $R_{1/2}A_{1/2}MnO_3$. We have used the RIETAN-97β program,[12] and have analyzed the neutron powder patterns at room temperature. The obtained lattice parameters, as well as oxygen occupancy, at room temperature are listed in Table I. We also

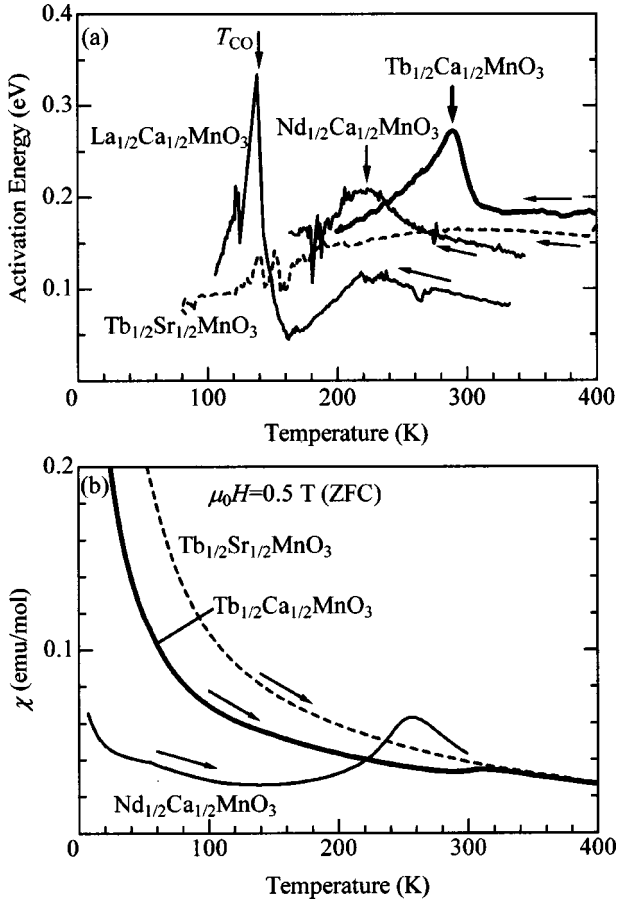

FIG. 1. Temperature dependence of (a) activation energy E_{ac} [$\equiv d(\ln\rho)/d(1/T)$; ρ is resistivity] and (b) susceptibility χ for $R_{1/2}A_{1/2}MnO_3$. χ was measured after cooling down to 5 K in the zero field (ZFC). Downward arrows indicate the critical temperatures T_{CO} for the charge-ordering transition, determined from the maximal point of the E_{ac}-T curve.

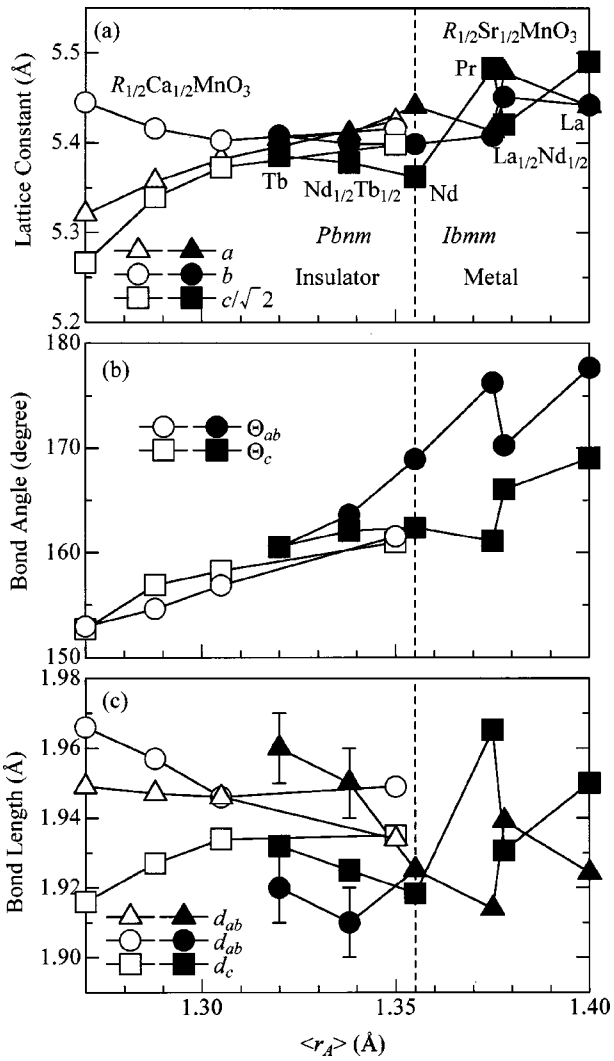

FIG. 2. Variation of structural parameters for $R_{1/2}A_{1/2}MnO_3$ against averaged ionic radius $\langle r_A\rangle$ of the perovskite A site: (a) lattice constants, (b) Mn-O-Mn angles, Θ_{ab} and Θ_c, (c) Mn-O bond lengths, d_{ab} and d_c. Open and closed symbols stand for the Ca and Sr compounds, respectively. Except for $Tb_{1/2}Sr_{1/2}MnO_3$ and $(Nd_{1/2}Tb_{1/2})_{1/2}Sr_{1/2}MnO_3$ [see (c)], error bar for the bond angles [(b)] and bond lengths [(c)] is less than 0.2° and 0.004 Å, respectively.

listed T_{CO} and T_C, which were determined from temperature dependence of E_{ac} and magnetization M, respectively. Figure 2 shows thus obtained structural parameters against $\langle r_A\rangle$: (a) lattice constants, (b) Mn-O-Mn angles Θ, and (c) Mn-O bond lengths d. Open and closed symbols stand for the Ca and Sr compounds, respectively. Variation of the lattice constants a, b, and $c/\sqrt{2}$ [Fig. 2(a)], as well as of the Θ values [Fig. 2(b)] is nearly scaled to $\langle r_A\rangle$ irrespective of the alkaline-earth species. Note that there are two Mn-O-Mn angles, i.e., out-of-plane (Θ_c, square) and in-plane (Θ_{ab}, circle) angles, in the *Pbnm* setting. The averaged Θ value increases almost linearlly with $\langle r_A\rangle$: $\langle\Theta\rangle=-34+148\langle r_A\rangle$. A similar interrelation between $\langle\Theta\rangle$ and $\langle r_A\rangle$ has been reported by Radaelli *et al.*[1] at $x=0.3$: $\langle\Theta\rangle=-7+124\langle r_A\rangle$. Here, $La_{1/2}Sr_{1/2}MnO_3$, $Pr_{1/2}Sr_{1/2}MnO_3$, and $(La_{1/2}Nd_{1/2})_{1/2}Sr_{1/2}MnO_3$ are known to be metallic[19] down to the lowest temperature, due to the large Θ value, or the large one-electron bandwidth W.

Now, let us proceed to the distortion of the MnO_6 octahedra of the insulating manganites. In the *Pbnm* setting, there are three kinds of Mn-O bonds, i.e., out-of-plane (d_c, square) and in-plane (d_{ab}, circle and triangle) bonds. In the four Ca compounds, i.e., $La_{1/2}Ca_{1/2}MnO_3$, $Nd_{1/2}Ca_{1/2}MnO_3$, $(Nd_{1/2}Tb_{1/2})_{1/2}Ca_{1/2}MnO_3$, and $Tb_{1/2}Ca_{1/2}MnO_3$, d_c is the shortest among the three bond lengths. With this structure, the $d_{3x^2-r^2}$ and $d_{3y^2-r^2}$ orbitals are stable as compared with the $d_{3z^2-r^2}$ orbital. Then, the e_g electrons tend to occupy the $d_{3x^2-r^2}$ and $d_{3y^2-r^2}$ orbitals, and hence, are easy to form the $d_{3x^2-r^2}/d_{3y^2-r^2}$ orbital alternation at low temperatures to cause the charge-ordering transition. By contrast, in $(Nd_{1/2}Tb_{1/2})_{1/2}Sr_{1/2}MnO_3$ and $Tb_{1/2}Sr_{1/2}MnO_3$, one of the d_{ab} is the longest. Such a Jahn-Teller-type distortion of the MnO_6 octahedra fairly destabilizes the orbital alternation, which is indispensable to the charge-ordering transition of the half-doped manganites.

To quantitatively estimate the stability of the respective e_g orbital, we have calculated the Madelung potential V for each orbital[20] based on the structural data. The Madelung potential acting on a hole in the $d_{3x^2-r^2}$, $d_{3y^2-r^2}$, and $d_{3z^2-r^2}$ orbitals is given by

$$V(d_{3x^2-r^2})=[V(\vec{r}_0+r_d\hat{x})+V(\vec{r}_0-r_d\hat{x})]/2, \qquad (1)$$

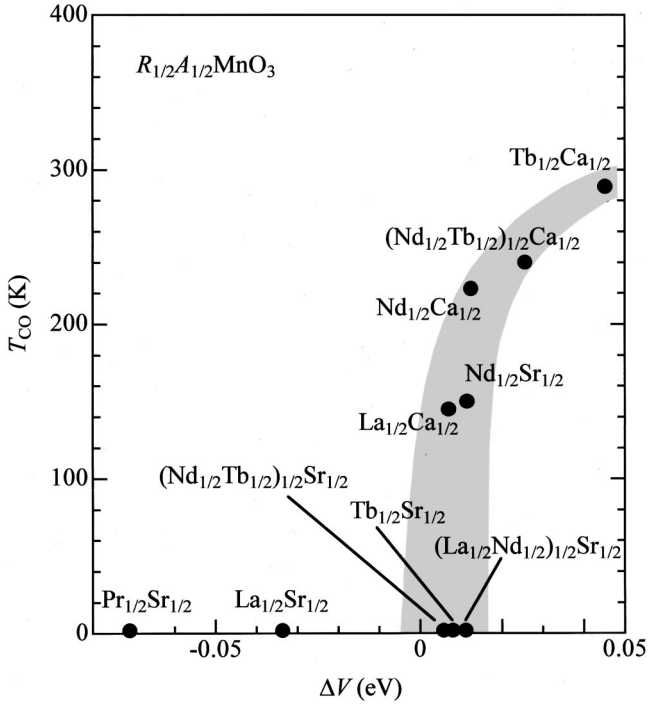

FIG. 3. Critical temperature T_{CO} for the charge-ordering transition for $R_{1/2}A_{1/2}MnO_3$ against the difference of the Madelung energies $\Delta V(\equiv[V(d_{3x^2-r^2})+V(d_{3y^2-r^2})]/2-\langle V\rangle)$. $\langle V\rangle$ is the averaged value for the three orbitals: $d_{3x^2-r^2}$,$d_{3y^2-r^2}$, and $d_{3z^2-r^2}$. Hatching is a guide to the eye.

$$V(d_{3y^2-r^2})=[V(\vec{r}_0+r_d\hat{y})+V(\vec{r}_0-r_d\hat{y})]/2, \tag{2}$$

and

$$V(d_{3z^2-r^2})=[V(\vec{r}_0+r_d\hat{z})+V(\vec{r}_0-r_d\hat{z})]/2, \tag{3}$$

respectively. Here, $\vec{r}_0$ indicates the position of the Mn ion and r_d $(=0.42$ Å) is the radius where the radial charge density of the Mn $3d$ orbital becomes maximum. $\hat{x}$,$\hat{y}$, and $\hat{z}$ are the unit vectors along the respective Mn-O bond directions. The magnitudes of the charge at A, Mn, and oxygen sites are assumed to be $+2.5$,$+3.5$, and -2, respectively, and the conventional Ewald method is used. The larger V is, the more stable the corresponding orbital becomes. The stability of the $d_{3x^2-r^2}/d_{3y^2-r^2}$ orbital alternation can be estimated by the difference of the Madelung potential ΔV:

$$\Delta V=[V(d_{3x^2-r^2})+V(d_{3y^2-r^2})]/2-\langle V\rangle. \tag{4}$$

Here, $\langle V\rangle(\equiv[V(d_{3x^2-r^2})+V(d_{3y^2-r^2})+V(d_{3z^2-r^2})]/3)$ is the averaged value. We plotted in Fig. 3 the charge-ordering temperature T_{CO} against ΔV. If one sees the phase diagram from left to right (the stability of the $d_{3x^2-r^2}/d_{3y^2-r^2}$ orbital alternation increases), the CO state appears and T_{CO} increases. Thus, the orbital stability is an important factor for the charge-ordering transition in the structure-controlled half-doped manganites.

Finally, let us compare the lattice effects of the present cubic system with those of the layered manganites. In the layered manganites, chemical substitution scarcely alters the in-plane Mn-O bond length d_{in} or the in-plane Mn-O-Mn angle Θ_{in}, and hence does not alter the in-plane t value: for example, $\Theta_{in}(d_{in})$ is 178.9° (1.934 Å) for $La_{1.2}Sr_{1.8}Mn_2O_7$ and 176.7° (1.929 Å) for $(La_{0.6}Nd_{0.4})_{1.2}Sr_{1.8}Mn_2O_7$.[3] The chemical pressure, on the other hand, changes the position of the apical oxygen, and modifies the orbital stability via deformation of the MnO_6 octahedra. In fact, a lattice effect observed in several layered systems, e.g., $(La,Nd)_{0.5}Sr_{1.5}MnO_4$ (Ref. 2) and $(La,Nd)_{1.2}(Sr,Ca)_{1.8}Mn_2O_7$,[3,21] has been ascribed to the variation of the orbital stability. Even in the cubic system, orbital stability plays an important role on the charge/orbital-ordered state of the half-doped manganites.

This work was supported by a Grant-in-Aid for Scientific Research from the Ministry of Education, Science, Sports and Culture, Japan.

[1] H.-Y. Hwang *et al.*, Phys. Rev. Lett. **75**, 914 (1995); P.G. Radaelli *et al.*, Phys. Rev. B **56**, 8265 (1997).
[2] Y. Moritomo *et al.*, Phys. Rev. B **56**, 14 879 (1997).
[3] T. Akimoto *et al.*, Phys. Rev. B **59**, R14 153 (1999); **61**, 11 270 (2000).
[4] H. Kuwahara *et al.*, Science **270**, 961 (1995).
[5] E.O. Wollan and W.C. Koehler, Phys. Rev. **100**, 545 (1955); J. B. Goodenough, *ibid.* **100**, 564 (1955).
[6] H. Kawano *et al.*, Phys. Rev. Lett. **78**, 4253 (1997); R. Kajimoto *et al.*, Phys. Rev. B **60**, 9506 (1999).
[7] P.G. Radaelli *et al.*, Phys. Rev. B **55**, 3015 (1997).
[8] K. Nakamura *et al.*, Phys. Rev. B **60**, 2425 (1999).
[9] S. Mori *et al.*, Nature (London) **392**, 473 (1998).
[10] See, for example, Y. Moritomo *et al.*, Phys. Rev. B **55**, 7549 (1997).
[11] H. Kuwahara *et al.*, Phys. Rev. B **56**, 9386 (1997).
[12] F. Izumi, in *The Rietveld Method*, edited by R. A. Young (Oxford University Press, Oxford, England, 1993), Chap. 13; Y.-I. Kim and F. Izumi, J. Ceram. Soc. Jpn. **102**, 401 (1994).
[13] K. Ohoyama *et al.*, Jpn. J. Appl. Phys., Part 1 **37**, 3319 (1998).
[14] J. Blasco *et al.*, J. Phys.: Condens. Matter **9**, 10 321 (1997).
[15] J. Fontcuberta *et al.*, Phys. Rev. B **60**, 6266 (1999).
[16] A. Sundaresan *et al.*, Phys. Rev. B **55**, 5596 (1997).
[17] N.V. Kasper *et al.*, J. Phys.: Condens. Matter **9**, 7455 (1997).
[18] B. Gracía-Landa *et al.* [J. Appl. Phys. **83**, 7664 (1998)] have observed anomalies in magnetic behavior of $Gd_{1/2}Sr_{1/2}MnO_3$, and ascribed it to charge-ordering transition. Judging from $\langle r_A\rangle$ dependence of T_{CO} in the Sr-based compounds, however, the anomalies are considered to be ascribed to the spin-glass transition.
[19] T. Akimoto *et al.*, Phys. Rev. B **57**, R5594 (1998).
[20] S. Ishihara *et al.*, J. Phys. Soc. Jpn. **66**, 2965 (1997).
[21] Y. Moritomo *et al.*, Phys. Rev. B **56**, R7057 (1997).